



ELSEVIER

Tectonophysics 261 (1996) 179–192

TECTONOPHYSICS

## Possible mechanisms of dynamic nucleation and arresting of shallow earthquake faulting

Yasuhiro Umeda<sup>a</sup>, Teruo Yamashita<sup>b,\*</sup>, Taku Tada<sup>b</sup>, Nobuki Kame<sup>b</sup>

<sup>a</sup> Disaster Prevention Research Institute, Kyoto University, Gokasho Uji, Kyoto, Japan

<sup>b</sup> Earthquake Research Institute, University of Tokyo, 1-1-1 Bunkyo-ku Tokyo, Japan

Received 16 May 1995; revised version received 20 September 1995; accepted 20 September 1995

### Abstract

The nucleation and arresting mechanisms of large shallow earthquakes are investigated from both observational and theoretical viewpoints. We show that two distinct phases are commonly observed at the initial part of seismograms of large shallow earthquakes. The first phase denotes the onset of the P wave, which shows a very gradual increase in amplitude with time. This gradual change is interrupted by the arrival of the second phase, which causes an abrupt change in the amplitude. Our seismological observation shows that the time interval between the onset of the two phases is strongly correlated with the magnitude of the earthquake.

It is probable that the above two phases are related to some aspect of inhomogeneities in the earth's crust. One of the important sources of such inhomogeneities is known to be preexisting cracks and their interactions. We theoretically show in this paper that a rupture occurring in a zone of densely distributed cracks radiates elastic waves that can simulate the features of the above two phases; note that such a rupture is considerably affected by crack interactions. Theoretical calculation is also carried out to investigate the effect of crack interactions on the arresting of rupture propagation. A propagating crack can excite subsidiary cracks ahead of its crack tip, which gives rise to crack interactions. We show that these interactions sometimes facilitate the arresting of rupture propagation.

### 1. Introduction

One of the empirical relations well established in seismology is the Gutenberg–Richter relation, a power law that relates frequency distribution of earthquake sizes with the seismic moment. This relation implies that a nucleated event very rarely grows into a large one. In recent years, there has been much effort to try to understand the underlying mechanism of the Gutenberg–Richter relation on the basis of

the concept of self-organized criticality (e.g., Bak and Tang, 1989; Carlson and Langer, 1989; Rice, 1993; Yamashita, 1993). However, it is not yet understood why only few events grow into large ones and whether the growth into a large event is pre-determined at the nucleation stage of the event. To challenge the problem of the difference in the growth process of large and small earthquakes, we have to study not only the nucleation mechanism, but also the arresting mechanism of earthquake faulting.

It has recently become possible to detect a phase in seismograms associated with the dynamic nucleation of large shallow earthquakes due to the instal-

\* Corresponding author. Fax: +81-3-3816-1159; e-mail: tyama@eri.u-tokyo.ac.jp.

lation of seismographs with sufficient dynamic range and bandwidth (Umeda, 1990, 1992; Ellsworth and Beroza, 1995). We will show in this paper on the basis of our seismological observations of such nucleation phase (Umeda, 1990, 1992) that it is likely that slow preliminary rupture growth commonly takes place at the dynamic nucleation stage of large shallow earthquakes. We will also show that the growth into a large event seems to be predetermined during the dynamic nucleation process of an earthquake.

We will investigate in this paper the nucleation and arresting mechanisms of large shallow earthquakes on both theoretical and observational grounds. We will show that crack interactions play a crucial role in earthquake ruptures from their nucleation to arresting; the slow preliminary rupture process can also be understood as a manifestation of the crack interactions. It seems that crack interaction provides a key to understand in a unified way many seemingly diverse aspects of shallow earthquake ruptures.

## 2. Dynamic nucleation process of large shallow earthquakes

According to our classification based on seismological observations, it seems that the rupture process of a large shallow earthquake is generally composed of the following three stages in the order of time (Umeda, 1990, 1992; Yamashita and Umeda, 1994): (1) a relatively slow and smooth preliminary rupture process; (2) a relatively large event characterized by the radiation of seismic waves enriched with high-frequency components; and (3) formation of the entire fault and the arresting of rupture propagation. The first two stages have been identified in the seismograms owing mainly to the recent installation of seismographs with sufficient dynamic range and bandwidth.

The initial part of vertical seismograms of the main shock of the 1984 Western Nagano earthquake is shown in Fig. 1 as an example. We can observe the low-frequency, low-amplitude waves marked by the symbol  $P_1$ , and high-frequency, high-amplitude waves marked as  $P_2$ ; these two phases are identified for this earthquake on the seismograms recorded at various stations at different epicentral distances and azimuths (Fig. 1). It was confirmed that these two phases have their origin at the earthquake source

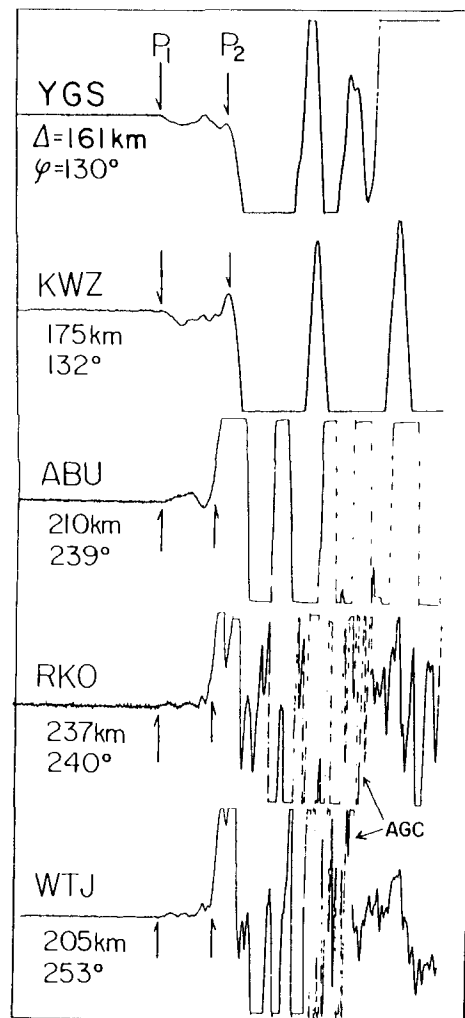


Fig. 1. Vertical seismograms near the arrival times of P waves emitted from the main shock ( $M = 6.8$ ) of the 1984 Western Nagano earthquake (after Umeda, 1990). AGC denotes auto-gain control. Epicentral distance and azimuth of each station are shown by  $\Delta$  and  $\phi$ , respectively.

(Umeda, 1990). These two distinct phases have also been found for many large shallow earthquakes by Umeda (1990, 1992).

The existence of the second phase,  $P_2$ , is also supported for large shallow inland earthquakes, by conspicuous field evidences such as dense distribution of surface cracks and high acceleration occasionally exceeding the earth's gravity (Umeda, 1981, 1992; Umeda et al., 1987). An evidence of such high acceleration comes from the observation of a

number of boulders thrown up by severe shaking; for example, it was observed in the 1990 Philippine earthquake that a boulder with dimensions of  $40 \times 27 \times 18 \text{ cm}^3$  had been tossed up and landed upside down at a distance of 45 cm from its original socket (Umeda, 1992). Under a simple assumption, the ground movements can be estimated from the dislodgment distance of this boulder; in the frequency range of 1–5 Hz, the ground velocity and acceleration were estimated to be 1.3–3.0 m/s and 1.6–4.7 g, respectively, by Umeda et al. (1991). The region characterized by such features as densely distributed cracks and high acceleration is found to be fairly small in comparison with the total rupture area. Umeda (1990) termed this small region the *earthquake bright spot*; an example of the earthquake bright spot is shown in Fig. 2 observed in the 1989 Loma Prieta earthquake. It is noteworthy that this bright spot is located precisely above the source of the strongest high-frequency radiation that was determined by Zeng et al. (1993) using the strong motion data.

It is likely that the two phases,  $P_1$  and  $P_2$ , represent two qualitatively different rupture stages during

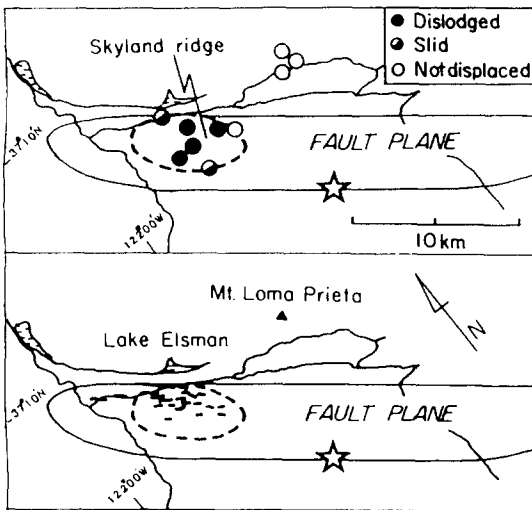


Fig. 2. The earthquake bright spot found for the 1989 Loma Prieta, California, earthquake (the zone surrounded by the broken curve), which is characterized as a zone of high ground acceleration and densely distributed surface cracks. The upper and lower figures show the distributions of dislodged boulders and surface cracks, respectively. The star stands for the epicenter of the main shock.

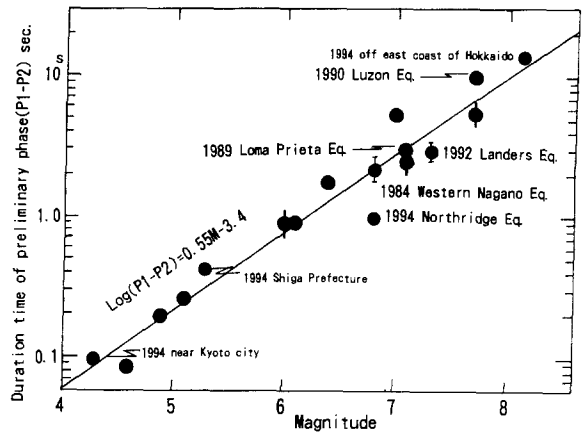


Fig. 3. Relation between the duration time of the preliminary rupture phase and the earthquake magnitude.

the dynamic nucleation of a larger shallow earthquake. Here, the term dynamic nucleation of earthquake rupture stands for the initial growth stage of earthquake rupture that radiates seismic waves. We define the time interval between the onset of the two phases  $P_1$  and  $P_2$  as the *preliminary rupture phase*, and denote its duration as  $t_n$ ; the phase beginning with  $P_2$  is termed the *bright spot phase* since it seems to be closely related to the formation of the earthquake bright spot. We have found a strong correlation between the duration time of the preliminary rupture phase,  $t_n$  (in seconds), and the eventual magnitude  $M$  of the earthquake in the form:

$$M = 1.92 \log t_n + 6.18 \quad (1)$$

by analyzing seismograms of many shallow earthquakes (Fig. 3); five new data are now added to the data set compiled by Umeda (1992). It is found that relation (1) is valid over a fairly wide magnitude range. This relation gives important implications for the growth process of large shallow earthquakes. It is inferred from Eq. (1) that the final rupture size is not predetermined at the very inception of dynamic earthquake rupture; the future rupture size is determined only after the advent of the bright spot phase.

### 3. The fundamental mechanisms of crack interactions

It is probable that the two phases, the preliminary rupture phase and bright spot phase, are related to

some aspect of the irregularity of the earthquake ruptures. One of the major sources of the irregularities is preexisting defects in the earth's crust such as cracks and faults (Yamashita and Umeda, 1994; Yamashita and Fukuyama, 1996). If cracks are densely distributed near an earthquake source, intense crack interactions are expected to occur in the earthquake rupture. These interactions give rise to a complex rupture process as will be discussed below in this section. In fact, the active part of a fault is known to form a fault zone, and it is generally considered as a region of increased crack density compared to the nearby crust (e.g., Rice, 1992; Leary et al., 1987). Leary et al. (1987) analyzed borehole seismograms recorded in the vicinity of an active fault in California, and showed that cracks are aligned predominantly parallel to the fault plane and the crack density increases with approaching the fault plane. Hence it is likely that the crack interaction plays a crucial role in an earthquake rupture from its nucleation to arresting. Yamashita and Umeda (1994), in fact, showed in their numerical analysis that the crack interactions give rise to irregular dynamic rupture propagation.

The crack interactions mainly depend on the geometrical configuration of the cracks. The fundamental mechanisms of the dynamic crack interactions can be inferred to some extent from the static analysis of two interactive cracks and of an isolated crack. It is known from the static analysis of an isolated shear crack that the shear stress is enhanced outside the crack near the tips, whereas it is lowered to the residual stress level near the crack trace. The stress field around two interactive cracks can be inferred from the stress change observed for the isolated crack. When the two cracks are coplanar and close to each other as illustrated in Fig. 4a, much higher stress should be observed in the narrow zone between the inner tips of the two cracks than in the absence of the interactions because the inner crack tips are located in the stress increase zone formed by each other crack. Hence catastrophic rupture is expected to take place at the inner crack tips. On the other hand, when two nearby cracks are non-coplanar and overlapped as illustrated in Fig. 4b, the stress near the inner crack tips should be much lower than in the absence of the interactions: the inner tips are located in the stress decrease zone formed by each other

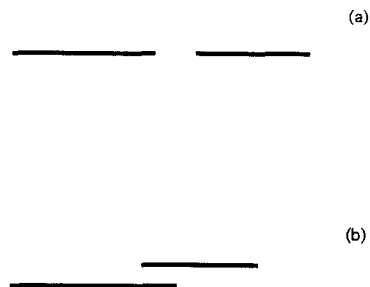


Fig. 4. Two close parallel cracks. (a) coplanar cracks, (b) non-coplanar cracks.

crack. The stress decrease zone near a crack trace is referred to as the stress shadow in this paper after the terminology of Yamashita and Umeda (1994). Hence the occurrence of catastrophic rupture at the inner tips tends to be suppressed in the configuration such as illustrated in Fig. 4b. If one of the two cracks lies entirely in the stress shadow of the other, the growth of the former is almost entirely suppressed and the interaction is almost unilateral from the latter to the former. Rigorous static analysis of two interactive cracks shows that the above qualitative consideration is fundamentally correct (e.g., Yamashita, 1995).

The above consideration on the modes of crack interactions qualitatively holds true even in the dynamic interactions among parallel cracks. Yamashita and Umeda (1994) numerically studied the dynamic interactions among propagating parallel antiplane cracks, and showed that if a propagating tip of a crack enters the stress shadow of a neighboring non-coplanar crack, the propagation is decelerated; the arresting of propagation may occur if the dimension of the stress shadow is large enough and/or the stress level is sufficiently low in the stress shadow. Hence the existence of neighboring non-coplanar cracks can be a cause of deceleration of the dynamic crack growth. On the other hand, if a crack exists ahead of a propagating crack tip on the same plane, then the growth rate is accelerated as both cracks approach each other, and coalescence occurs. Hence the coplanar interaction can be a cause of acceleration of dynamic crack propagation. If cracks are densely distributed in a zone, the above-stated two conflicting modes of interaction coexist, which makes the dynamic rupture process highly complex.

#### 4. A theoretical model for the dynamic nucleation of earthquakes in a fault zone

As stated before, the active part of a fault is generally considered as a region of increased crack density compared to the nearby crust. It is therefore expected that the crack interactions play a crucial role in the nucleation stage of an earthquake. Yamashita and Knopoff (1989, 1992), in fact, successfully explained the seismic quiescence and foreshock occurrence on the basis of multiple interactions among densely distributed cracks. It will be shown in this section that the crack interactions play an important role in the dynamic nucleation of earthquake rupture as well.

In this section we review the study of Kame (1995), who proposed a new model for the dynamic nucleation of earthquake rupture. He theoretically analyzed the dynamic rupture nucleation in a zone where parallel preexisting antiplane Griffith cracks are densely distributed; the medium is assumed to be elastic, homogeneous, isotropic, and infinite. The details of the analysis and the results of the calculations shall be described in a forthcoming paper by Kame and Yamashita (1996). A typical example of the assumed cracked zone is illustrated in Fig. 5. The use of such a cracked zone model is justified because densely distributed small cracks are expected in fault zones as stated before, and the cracks are known to be aligned predominantly parallel to the fault plane; in addition, it is expected that the preexisting cracks have quasistatically grown up into larger ones, due to stress corrosion cracking, at the epicentral area of

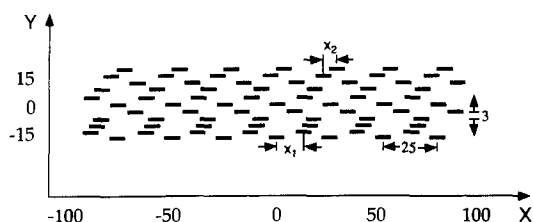


Fig. 5. An example of the assumed cracked zone, which is a model of a fault zone; each line segment denotes a crack. All the cracks are assumed to have the same length 7.0. In this example, we fix the spacing of the crack centers at 25.0 on each crack array, and the crack array spacing at 3.0. However, the relative location of the cracks in the  $X$ -direction on different arrays, such as  $x_1$  or  $x_2$ , is assumed to obey a homogeneous random distribution. The first dynamic growth occurs at the crack whose center is at  $X = 0$  and  $Y = 0$ .

the eventual earthquake immediately before its occurrence (Yamashita and Knopoff, 1992). Note that the effect of non-coplanar interactions is relatively dominant in the crack distribution assumed in the example shown in Fig. 5: the crack spacing is much smaller in the  $Y$ -direction than in the  $X$ -direction, where  $X$  and  $Y$  are the nondimensional coordinates given by  $X = x/L$  and  $Y = y/L$ , respectively (see Appendix A). Kame (1995) rigorously treated the dynamic multiple interactions among the cracks, using the boundary integral equation method originally developed by Cochard and Madariaga (1994) for the analysis of an isolated crack and later extended by Yamashita and Fukuyama (1996) to incorporate the case of multiply interactive cracks. The boundary integral equation method used therein is reviewed in Appendix A.

Kame (1995) assumed the critical stress fracture criterion for the analysis of spontaneous crack propagation as in Yamashita and Umeda (1994). In other words, a crack is assumed to begin dynamic extension if the stress at the crack tip exceeds the assumed critical threshold. The critical threshold stress is assumed to be constant everywhere except near the tips of one of the cracks where slightly lower critical stress is assumed so as to enable the initiation of dynamic crack propagation there. The remotely applied load is assumed to be constant. The residual stress is also assumed to be constant on all the cracks, so that relative slip can occur freely due to the crack interactions so as to satisfy the constant residual stress boundary condition.

A typical example of the velocity seismogram due to rupture propagation in the cracked zone shown in Fig. 5 is plotted in Fig. 6; the velocity is recorded outside the cracked zone. It is observed in the calculation that the rupture initiated at the crack whose center is located at  $X = 0$  and  $Y = 0$  propagates on its plane, so that the rupture growth occurs in the form of dynamic coalescence of coplanar cracks (see Fig. 7). We also plot in Fig. 6 the velocity seismogram for the case when no non-coplanar interaction is taken into account; in other words, as the model for distributed cracks, we pick up only the array of coplanar cracks at  $Y = 0$  out of those shown in Fig. 5. We find a remarkable contrast between the two velocity seismograms in Fig. 6; the onset of the velocity wave is much more gradual when the cracks

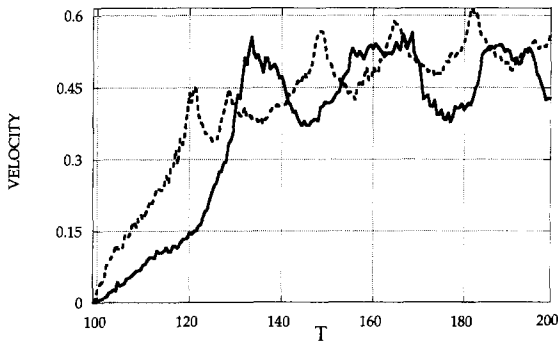


Fig. 6. Velocity seismograms recorded outside the cracked zone at  $X = 20$  and  $Y = 100$ . The ordinate denotes the nondimensional velocity  $dU/dT$ , where  $U$  and  $T$  are the nondimensional displacement and time, respectively (see Appendix A). The solid curve stands for the velocity radiated by the rupture in the cracked zone shown in Fig. 5. Only the coplanar crack array at  $Y = 0$  is taken into account in the calculation of the velocity illustrated by the broken curve. High-frequency oscillation is due to numerical errors.

are zonally distributed. Hence, it would be possible to attribute the preliminary rupture phase shown in Fig. 1 to the effect of the non-coplanar interactions in a fault zone.

We now consider in detail the mechanism of the gradual onset of the velocity wave such as shown in Fig. 6, following the studies of Kame (1995) and Kame and Yamashita (1996). For this purpose, the qualitative consideration of the two interactive static cracks, which were made in the preceding section, is helpful. As stated before, the crack interactions exert two conflicting effects: one tends to accelerate the crack growth, and the other to decelerate it. The accelerating and decelerating effects are generally ascribable to the coplanar and non-coplanar interactions, respectively. Thus the gradual buildup at the onset of the velocity wave shown by the solid curve in Fig. 6 can be claimed to be due to the relative predominance of the non-coplanar interactions at the initial stage of the rupture. The correctness of this inference is ascertained in comparison between the solid and broken curves because no gradual phase is observed at the onset of velocity wave when the crack distribution is only coplanar. This view is also justified by the ray theoretical calculation of the arrival time of elastic wave radiated by the rupture. It can be shown in this calculation that the abrupt increase in the time derivative of velocity (solid curve)

at time  $T(\equiv \beta t/L) \approx 123$  is emitted by the acceleration in crack growth rate due to the approach of the first nucleated crack to the neighboring cracks on both sides and their coalescence at  $T = 25$ – $27$  (see Fig. 7); note that crack growth is accelerated when two cracks come close to each other because coplanar interaction begins to prevail. Hence the abrupt change at  $T \approx 123$  is interpreted to be due to the transition from the state of non-coplanar interaction predominance to that of coplanar interaction predominance.

The above considerations suggest that the gradual onset of the velocity waves will not be observed when coplanar interactions are dominant in the pre-existing cracks even if the cracks are distributed in a zone. This expectation turned out to be in fact the case in the model calculations of Kame (1995). However, from the seismological viewpoint, it seems more reasonable to assume that non-coplanar crack interactions are dominant before the occurrence of a large shallow earthquake. The existence of a pe-

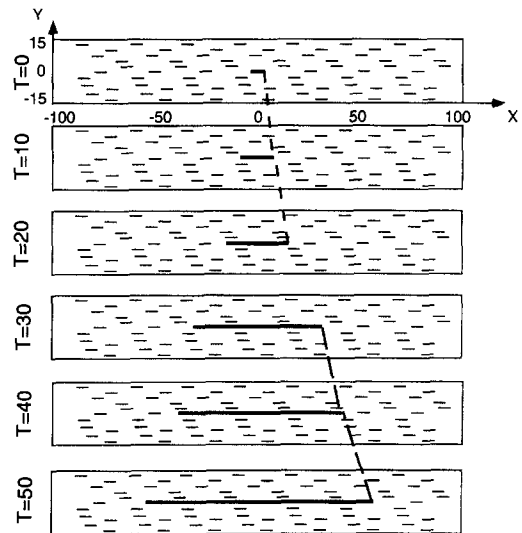


Fig. 7. Snap shot of rupture propagation in the cracked zone shown in Fig. 5. The propagating and stationary cracks are shown by the thick and thin line segments. The first coalescence is done with the neighboring crack on the left at  $T \approx 25.0$ . The growth rate of the right tip of the propagating crack can be estimated from the slope of the broken line, which stands for the spatio-temporal growth of the right crack tip. We note that the growth rate  $v$  is very low at the inception of the rupture:  $v \approx 0.5\beta$  and  $\approx 0.9\beta$  for  $0 < T < 20$  and for  $30 < T < 50$ , respectively.

riod of seismic quiescence before the occurrence of a large shallow earthquake in its epicentral region (Allen et al., 1965; Fedotov, 1965; Mogi, 1969; Ohtake, 1976; Ohtake et al., 1977) suggests that the rupture occurrence is totally suppressed in the future epicentral area in this time period. We can therefore infer that non-coplanar crack interactions are dominant in the period of seismic quiescence as long as the cracked zone model is appropriate. In fact, Yamashita and Knopoff (1992) showed in their simulations that the dominance of non-coplanar crack interactions causes seismic quiescence before the occurrence of a large event.

Umeda (1990) showed that the preliminary rupture phase is not observed for aftershocks even if they are large enough (Fig. 8). This observation is consistent with our interpretation. Since a predominantly large fault appears with the occurrence of a main shock, the coplanar interactions will be dominant in the aftershock sequence. This does not cause the preliminary rupture phase in a seismogram of an aftershock according to our modeling results: in our model, non-coplanar interactions have to prevail before the occurrence of rupture for the appearance of the preliminary rupture phase.

Later abrupt changes in the velocity seismograms in Fig. 6 are associated with crack coalescence. For example, the abrupt increase at  $T \approx 145$  on the solid curve is due to the coalescence of the propagating crack with the cracks whose centers are at  $X = -52$  and  $X = 55$  on the line  $Y = 0$ : it is theoretically known that the dynamic crack coalescence can be a source of high-frequency elastic wave radiation (Madariaga, 1983). The decrease beginning at  $T \approx 134$  in the solid curve is caused by the temporary deceleration of crack growth just after the coalescence of the first nucleated crack with the neighboring cracks on both sides at  $T = 25-27$  (see Fig. 7): abrupt change in crack propagation velocity is known to be another source of high-frequency radiation (Madariaga, 1977; Yamashita, 1983). This deceleration will occur since the effect of coplanar crack interactions becomes temporarily less dominant just after the completion of crack coalescence.

The crack tip velocity generally accelerates with its growth and soon gets close to the S wave velocity, which is the maximum allowable velocity for an antiplane crack (Kostrov, 1966). Hence a larger change

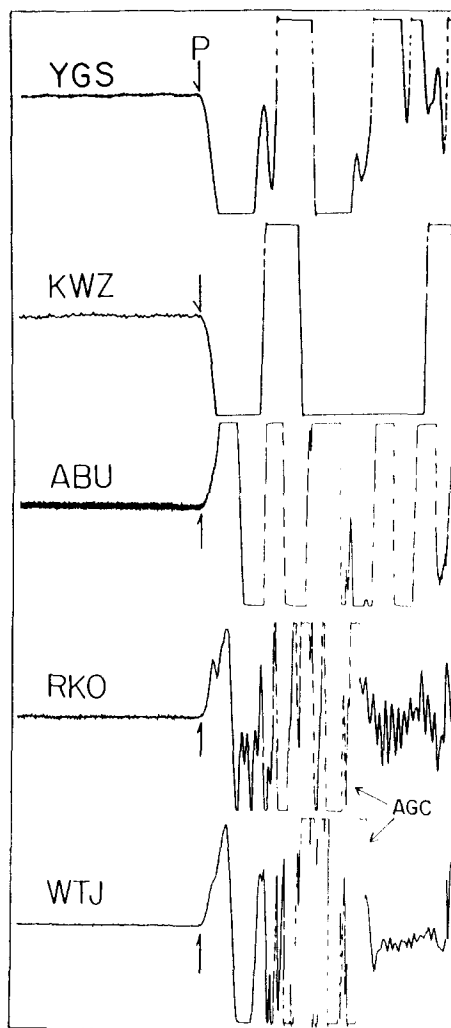


Fig. 8. Vertical seismograms emitted from an aftershock ( $M = 6.2$ ) of the 1984 Western Nagano earthquake (after Umeda, 1990). Note that the magnitude of this event is comparable to that of the main shock, whose seismograms are shown in Fig. 1.

in the crack tip velocity can occur due to crack coalescence at earlier stage of growth. This suggests that high-frequency acceleration can be efficiently radiated at the beginning stage of crack propagation since radiated energy of high-frequency acceleration is generally larger for a larger change in crack tip velocity (Madariaga, 1977; Yamashita, 1983). The accelerogram corresponding to the velocity seismogram shown in Fig. 6 is illustrated in Fig. 9 as an example; the highest acceleration is radiated by

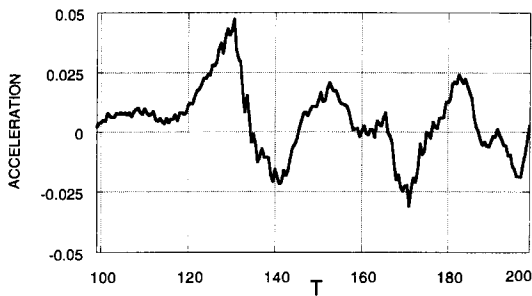


Fig. 9. Accelerogram corresponding to the velocity seismogram shown by the solid curve in Fig. 6.

the coalescence of the first nucleated crack with the neighboring cracks on both sides at  $T = 25$ – $27$  in this example (see also Fig. 7). The above consideration implies that an earthquake bright spot tends to be formed relatively close to the hypocenter, which is consistent with the seismological observations of Umeda (1990, 1992). This model for the earthquake bright spot marks an improvement over the model proposed by Yamashita and Umeda (1994), who argued that an earthquake bright spot can be formed when nucleation and propagation arresting of several cracks occur in any localized area, which does not necessarily have to be formed close to the hypocenter.

In summary, it is essential for the appearance of the slow preliminary rupture phase that non-coplanar interactions are dominant in zonally distributed pre-existing cracks. On the other hand, what is essential for the appearance of the bright spot phase is the excitation of dynamic slips, due to interactions, on cracks ahead of the crack where the first dynamic growth occurs. If no slips are excited on these cracks, the bright spot phase will not be observed because large sudden energy release does not occur at the coalescence with such cracks.

### 5. An arresting mechanism of dynamic propagation of earthquake ruptures

If the stress drop is positive over a propagating fault plane, the shear stress at the fault tip monotonically increases with the growth of the fault. Hence a large discontinuous increase in the fracture strength is inevitably required for the abrupt arresting of

fault propagation. Although many researchers have a priori assumed unbreakable barriers at the point of arresting, it is highly questionable that arresting of fault propagation occurs in such a way in the ordinary earth's crust materials once the fault has grown up to a significantly large size.

Once a crack begins dynamic propagation, its size soon becomes far larger than those of the preexisting cracks in the fault zone, thus being little affected by the latter. Hence it appears that a propagating crack can practically be treated as an isolated crack after the growth to a sufficiently large size. However, this is not necessarily the case since the propagating crack may dynamically excite cracks ahead of the propagating tip (e.g., Yamashita and Umeda, 1994). This dynamic crack excitation gives rise to a new kind of interaction. We now briefly investigate how these interactions affect the dynamic crack propagation on the basis of simple examples. The analysis in this section is developed originally in this paper. The boundary integral equation method summarized in the Appendix is used again in the calculations.

Suppose an infinite homogeneous isotropic elastic medium, which is at rest in static equilibrium for  $T \leq 0$ . The deformation is assumed to be antiplane strain as in the preceding section, and we assume that an isolated crack is first formed at  $T = +0$  in response to a remotely applied load. In this section, we do not take account of preexisting interactive cracks, which are irrelevant to the main concern of the present modeling. The stress drop is assumed to be positive and constant on each crack; in addition, the crack nucleated first at  $T = +0$  is assumed to propagate with a constant velocity  $v/\beta = 0.8$  for simplicity. All the cracks are the Griffith type cracks as in the preceding section.

First, a reference model with an isolated crack is considered; the crack is assumed to be nucleated at the origin on the  $X$ - $Y$  plane, and to propagate bilaterally on the  $X$ -axis (Fig. 10). We assume discontinuous increase in fracture strength at  $X = -8\Delta X$  and  $16\Delta X$ . Here,  $\Delta X$  is the size of the discretized elements on the crack trace, and it is assumed to be unity (see Appendix A). The strength barrier at  $X = -8\Delta X$  is assumed to be infinitely large, so that the crack can never propagate beyond this point; this means that we concentrate our attention only on rupture arresting at  $X = 16\Delta X$ . We can calculate the

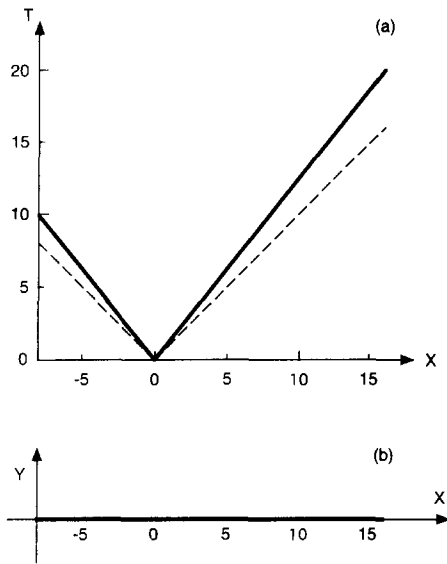


Fig. 10. (a) Spatio-temporal plot of the propagation path of the isolated crack with velocity  $v = 0.8\beta$  (solid line). The broken line denotes the front of S waves emitted by the dynamic nucleation of the crack. (b) The geometry of the crack at the instant when the propagation is arrested.

value of the minimum fracture strength required to arrest the propagation of this crack at  $X = 16\Delta X$ . Our main concern in the following calculations is about the effect of crack interactions on the minimum fracture strength required to arrest the rupture growth relative to this value, which is now defined as the relative minimum fracture strength.

We next consider the effect of excited subsidiary cracks on the arresting of rupture propagation. The crack first nucleated at  $T = +0$  is now referred to as the main crack. The main crack is assumed to be nucleated at the same location and to propagate with the same velocity as the isolated crack treated in Fig. 10. The main crack propagates as an isolated crack for a while until it excites subsidiary cracks. Let us first assume that the subsidiary cracks stop propagation soon after the nucleation, and the main crack continues to grow up to the discontinuity point  $X = 16\Delta X$ . This corresponds to a situation where the fracture strength is, on the average, higher on the planes of the subsidiary cracks than on the plane of the main crack (Yamashita and Umeda, 1994). Since the propagation velocity of the subsidiary cracks is generally smaller than that of main crack in such a

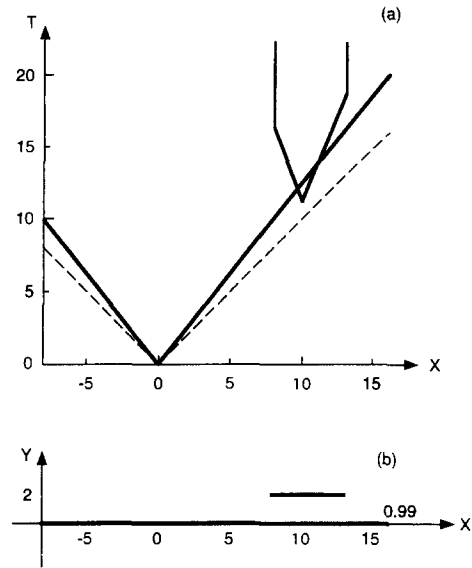


Fig. 11. (a) Spatio-temporal plot of the propagation paths of the main and subsidiary cracks (solid line). The broken line denotes the front of S waves emitted by the dynamic nucleation of the main crack. (b) The geometry of the cracks at the instant when the propagation of the main crack is arrested. The relative minimum fracture strength required to arrest the propagation of the main crack at  $X = 16\Delta X$  is 0.99.

situation (Yamashita and Umeda, 1994), we assume a lower rupture velocity of  $v/\beta = 0.4$  for them. All the subsidiary cracks are assumed to be excited at location  $X = 10\Delta X$  and at time  $T = 22.5\Delta T = 11.25$  soon after the arrival of the S waves emitted by the dynamic nucleation of the main crack (see Fig. 11a), where  $\Delta T$  is the nondimensional time increment, and  $\Delta T = 0.5$  is assumed (see Appendix A). We now consider two models for the distribution of the subsidiary cracks. A single subsidiary crack is excited in one of the models (Fig. 11), while two cracks are assumed in the other (Fig. 12); all the subsidiary cracks are assumed to be only  $2\Delta X$  apart

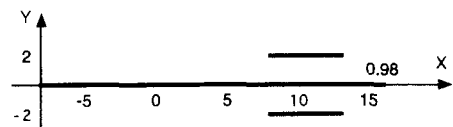


Fig. 12. The geometry of the cracks at the instant when the propagation of the main crack is arrested. The relative minimum fracture strength required to arrest the propagation of the main crack at  $X = 16\Delta X$  is 0.98. See Fig. 11b as to the spatio-temporal growth paths of the cracks.

from the main crack. The growths of the subsidiary cracks are assumed to be arrested at  $X = 8\Delta X$  and  $13\Delta X$  because the subsidiary cracks are entirely contained in the stress shadow formed by the main crack once the propagating tip of the main crack goes ahead of those of the subsidiary cracks. The results of the calculations show that the arresting of the main crack is more facilitated when the subsidiary cracks are excited; though the difference is not large. When the single subsidiary crack is excited, the relative minimum fracture strength required to arrest the propagation of the main crack is 0.99. The minimum strength is even smaller when the two subsidiary cracks are excited; the difference from the case of the isolated main crack is 2%. The facts observed above can be explained in terms of the decelerating effects of the non-coplanar crack interactions discussed in the preceding section. The strain energy released by the main crack in the range  $8\Delta X \leq X \leq 13\Delta X$  is smaller than when the main crack is isolated. This reduces the stress at the tips of the main crack. Hence we expect that the minimum fracture strength required to arrest the main crack propagation is lower if even more subsidiary cracks are excited.

We assumed in the calculations of Figs. 11 and 12 that the subsidiary cracks stop propagating soon after the nucleation. However, there is another possibility of the transfer of propagation from the main crack onto some of subsidiary cracks (Yamashita and Umeda, 1994). In other words, the main crack stops propagating soon after exciting subsidiary cracks, and some of the subsidiary cracks continue to propagate up to the discontinuity point  $X = 16\Delta X$ . This occurs when the fracture strength is, on the average, smaller on the planes of the subsidiary cracks than on the plane of the main crack (Yamashita and Umeda, 1994). We now treat this case, and investigate its effects on the arresting of rupture process. A single subsidiary crack is assumed to be excited in Fig. 13, while two such cracks are assumed in Fig. 14; all the subsidiary cracks in Figs. 13 and 14 are nucleated at the same location and time as in Figs. 11 and 12, respectively. Since the growth rates of the subsidiary cracks are expected to be larger in the present case than in the cases of Figs. 11 and 12, we assume the propagation velocity  $v/\beta = 0.8$  for both the subsidiary and main cracks. The growth of the right tip of the main crack is assumed to be

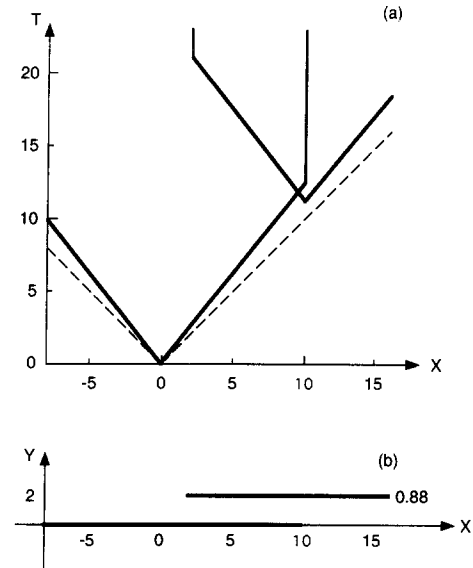


Fig. 13. (a) Spatio-temporal plot of the propagation paths of the main and subsidiary cracks (solid line). The broken line denotes the front of S waves emitted by the dynamic nucleation of the main crack. (b) The geometry of the cracks at the instant when the propagation of the subsidiary crack is arrested. The relative minimum fracture strength required to arrest the propagation of the subsidiary crack at  $X = 16\Delta X$  is 0.88.

arrested at  $T = 25\Delta T$  and  $X = 10\Delta X$  soon after entering the stress shadow formed by the subsidiary cracks on the basis of the findings by Yamashita and Umeda (1994) (see Fig. 13a): at the instance when the tip of the main crack enters the stress shadow formed by the subsidiary cracks, the dimension of the stress shadow is much larger in this situation than in the cases in Figs. 11 and 12. The propagation of the left tips of the subsidiary cracks are more easily arrested in this situation than that of the right tips if the other conditions are the same for the left and right tips because the left tips enter the stress shadow of the main crack (Yamashita and

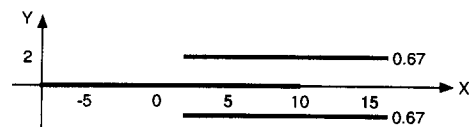


Fig. 14. The geometry of the cracks at the instant when the growths of the subsidiary cracks are arrested at  $X = 16\Delta X$ . The relative minimum fracture strength required to arrest the propagation of the subsidiary cracks is 0.67. See Fig. 13b as to the spatio-temporal growth paths of the cracks.

Umeda, 1994). Hence we assume in Figs. 13 and 14 that the left tips of the subsidiary cracks stop propagating at  $X = 2\Delta X$  in the stress shadow of the main crack. We now investigate the propagation behavior of the right tips of the subsidiary cracks at the discontinuity point  $X = 16\Delta X$ : note that the right tip of the main crack does not propagate up to this point. Our calculation shows that the relative minimum fracture strengths required to arrest the rupture propagation are 0.88 and 0.67, respectively, for the models in Figs. 13 and 14. The above simple calculation shows that the discontinuous transfer of the propagation (i.e., dynamic formation of a fault step) is much more effective for the arresting of rupture propagation than the cases when no transfer occurs. It is also observed that the arresting is much easier where more subsidiary cracks are excited. We assumed two subsidiary cracks at most. However, the minimum fracture strength will be even lower if more subsidiary cracks are assumed. Here, we have to note the stress at the right tips of the subsidiary cracks in Fig. 13 or 14 is much larger than when it is isolated because of the interaction between the main and subsidiary cracks. For example, our calculation shows that the relative minimum fracture strength required to arrest the rupture propagation at  $X = 16\Delta X$  is only 0.67 when the subsidiary crack in Fig. 13 is isolated.

In summary, the arresting of the rupture propagation is more facilitated if more subsidiary cracks are excited. A discontinuous transfer of the rupture further facilitates the arresting. Since the mechanical property of the shallow part of the earth's crust is thought to be very inhomogeneous, the excitation of subsidiary cracks is likely to occur.

## 6. What determines the size of shallow earthquakes?

The eventual size of an earthquake depends on how the fault propagation is arrested. The analysis in the preceding section shows that both excited subsidiary cracks and spatial inhomogeneity in fracture strength contribute to the arresting of rupture propagation. Hence fault propagation will be more easily arrested when it occurs in a region where the density of preexisting cracks is higher and/or the spatial inhomogeneity of fracture strength is higher.

The above interpretation is supported by the following seismological observations. It is known that mechanical heterogeneity is generally higher in volcanic regions and earthquakes occurring there are much smaller in size than tectonic earthquakes such as those at plate boundaries (e.g., Mogi, 1963). In addition, earthquake swarms tend to occur in regions where mechanical heterogeneity is high (Mogi, 1963); predominantly large events do not generally occur in earthquake swarms. High mechanical heterogeneity will be characterized by both high crack density and high inhomogeneity in the spatial distribution of fracture strength, so that the above observations are consistent with our interpretation.

## 7. Discussion and conclusions

We investigated in this paper the nucleation and arresting mechanisms of shallow earthquake faulting from both theoretical and observational viewpoints. We have found in our elaborate seismological observation the common existence of the preliminary rupture phase in many large shallow earthquakes. It was theoretically shown that crack interaction plays a certain role in the dynamic nucleation of shallow earthquake faulting. The preliminary rupture phase was explained in terms of non-coplanar crack interactions that tend to suppress the dynamic crack propagation. However, further study is required to quantitatively explain the relation (1).

Theoretical calculation is carried out to examine the effects of the crack interactions on the arresting of the rupture propagation. A propagating crack can excite subsidiary cracks ahead of the propagating tip after the crack has grown up to some extent, which complicates the overall rupture process through intense interactions (Yamashita and Umeda, 1994). It was shown that the rupture propagation can be arrested by a smaller discontinuity in fracture strength when subsidiary cracks are excited than when no subsidiary cracks are excited. The arresting of rupture propagation is generally easier when more subsidiary cracks are excited.

We assumed in the theoretical calculations that all the cracks are parallel and disconnected. This is a highly simplified assumption. For example, if two parallel cracks are close to each other and the inner crack tips are located outside the stress shadow of

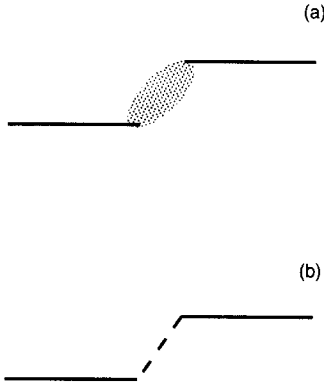


Fig. 15. Two non-coplanar cracks. Secondary fractures may occur in the shaded zone (a), or the two cracks may be connected as shown by the broken line (b).

each other crack as in Fig. 15, then connection of the two cracks, or the formation of many secondary fractures (Segall and Pollard, 1980) is very likely in the narrow zone between the inner crack tips. The effects of such phenomena will also have to be examined in future studies. Although we assumed only straight cracks in the present study, there is also a possibility of crack bifurcation. It is known from a static analysis that bifurcation can also reduce the stress singularity at crack tips (e.g., Sih, 1965), so that the bifurcation will also facilitate the fault propagation arresting. Crack configuration more complicated than treated in the present paper will be necessary for more realistic application of our concepts and for the understanding of the underlying mechanism of Eq. (1).

### Acknowledgements

Helpful comments were provided by R. Madariaga and an anonymous reviewer. This research was supported in part by a grant from the Ministry of Education, Science and Culture of Japan (project 06680423).

### Appendix A. Numerical analysis of dynamical growths of interactive cracks

We briefly review the method of analysis used by Yamashita and Fukuyama (1996), and Kame (1995), which is mostly based on the analysis of Cochard and Madariaga (1994).

Consider an infinite homogeneous elastic medium, which is at rest in static equilibrium for  $t \leq 0$ , and the deformation is assumed to be antiplane strain. When preexisting cracks are treated, we first assume instantaneous appearance of the cracks, and carry out the calculations in advance so that a stationary state has been reached by time  $t = 0$ .

The analysis is carried out in the time domain, and all the cracks are assumed to be aligned parallel. The dynamic displacement  $u$  is related to the relative slip on each crack by the convolution (Cochard and Madariaga, 1994):

$$u(x, y, t) = \sum_{j=1}^N \int_{\Gamma_j} \int_0^t \Delta u_j(\xi, \tau) F(x, y - y_j, \xi, t - \tau) d\xi d\tau, \quad (\text{A1})$$

where  $N$  is the number of cracks,  $\Delta u_j = u(x, y_j + 0, t) - u(x, y_j - 0, t)$  is the relative slip across the  $j$ th crack  $\Gamma_j$  ( $j = 1, \dots, N$ ),  $y_j$  is the  $y$  coordinate of the location of the  $j$ th crack, and  $F$  is the  $yz$  component of the stress tensor associated with the 2D displacement Green function:

$$G(x, y, \xi, t) = \frac{1}{2\pi\mu} \frac{H(t - r/\beta)}{\sqrt{t^2 - r^2/\beta^2}}, \quad (\text{A2})$$

where  $H(\cdot)$  is a unit step function,  $\beta$  is the shear wave velocity,  $\mu$  is the rigidity, and  $r = \sqrt{(x - \xi)^2 + y^2}$ . The stress component  $\sigma_{yz}$  is assumed to be given on each crack  $\Gamma_j$  ( $j = 1, \dots, N$ ) in the form:

$$\sigma_{yz}(x, y_j, t) = -\sigma_0 \quad (\text{A3})$$

as the boundary condition. We obtain the following integral equation on each crack by transforming Eq. (A1) (Cochard and Madariaga, 1994):

$$\begin{aligned} \sigma_{yz}(x, y, t) = & -\frac{\mu}{2\pi} \sum_{j=1}^N \left( \int_{\Gamma_j} \frac{x - \xi}{(x - \xi)^2 + (y - y_j)^2} d\xi \right. \\ & \times \int_0^t \frac{\partial}{\partial \xi} \Delta \dot{u}_j(\xi, \tau) \frac{t - \tau}{\sqrt{(t - \tau)^2 - r_j^2/\beta^2}} d\tau \\ & \left. + \frac{1}{\beta^2} \int_{\Gamma_j} d\xi \int_0^t \frac{\partial}{\partial \tau} \Delta \dot{u}_j(\xi, \tau) \frac{d\tau}{\sqrt{(t - \tau)^2 - r_j^2/\beta^2}} \right), \end{aligned} \quad (\text{A4})$$

where  $r_j = \sqrt{(x - \xi)^2 + (y - y_j)^2}$ , and the dot denotes the partial differentiation with respect to time  $\tau$ . The physical quantities are normalized by an arbitrary unit of length  $L$  and the rigidity of the medium  $\mu$  in the following calculations. The nondimensional coordinates are therefore given by  $X = x/L$ ,  $Y = y/L$ , and  $T = \beta t/L$ ; the stress and displacement by  $S = \sigma_{yz}/\mu$  and  $U = u/L$ . Eq. (A4) is discretized, using the technique developed by Cochard and Madariaga (1994). In this discretization, the nondimensional slip velocity is assumed to be uniform on a rectangular element on the  $XT$  plane with uniform spacing  $\Delta X$  in space and  $\Delta T$  in time. The stress  $S$  on the element  $X_i \leq X \leq X_{i+1} = X_i + \Delta X$  and  $T_k \leq T \leq T_{k+1} = T_k + \Delta T$  is evaluated at  $X = X_i + \Delta X/2$  and  $T = T_k + \Delta T$ . We set  $2\Delta T = \Delta X = 1$  in the calculations. We then get the discretized nondimensional integral equation:

$$S_{i,k}^j = -\frac{1}{2\pi} \sum_{l=1}^{N+1} \sum_{m=0}^k \sum_n V_{n,m}^l \Pi_{i-n,k-m}^{j-l} \quad (\text{A5})$$

on the crack surfaces after carrying out the integrations in Eq. (A4), where the summation with respect to  $n$  is done over the slipped area. Here  $S_{i,k}^j$  is the nondimensional stress at  $X = (i + 1/2)\Delta X$ ,  $Y = j\Delta X$  and  $T = (k + 1/2)\Delta X$  and  $V_{n,m}^l$  is the nondimensional slip velocity on the  $l$ th crack defined on the element  $X_n \leq X \leq X_{n+1}$  and  $T_m \leq T \leq T_{m+1}$ . When the element  $X = (i + 1/2)\Delta X$  and  $T = (k + 1/2)\Delta X$  lies within the wave cone, the expression for  $\Pi_{i,k}^j$  is given by:

$$\Pi_{i,k}^j = R_{i,k+1}^j - R_{i,k}^j - R_{i-1,k+1}^j + R_{i-1,k}^j, \quad (\text{A6})$$

where

$$R_{i,k}^j = \frac{i + 1/2}{(i + 1/2)^2 + j^2} \sqrt{k^2/4 - (i + 1/2)^2 - j^2} + \sin^{-1} \frac{i + 1/2}{\sqrt{k^2/4 - j^2}}. \quad (\text{A7})$$

If an element is crossed by the wave cone boundary, the integrations in Eq. (A4) must be carried out only inside the wave cone. When  $S_{i,k}^j$  is given on each crack surface as the boundary condition, the slip velocity is obtained from Eq. (A5) at any time step  $k$

in the form:

$$V_{i,k}^j = -\frac{2\pi}{\Pi_{0,0}^0} S_{i,k}^j - \frac{1}{\Pi_{0,0}^0} \sum_{l=1}^{N+1} \sum_{m=0}^{k-1} \sum_n V_{n,m}^l \Pi_{i-n,k-m}^{j-l} \quad (\text{A8})$$

where  $\Pi_{0,0}^0 = \pi$ . Once the slip velocity  $V_{i,k}^j$  is obtained, the emitted stress wave can be calculated from Eq. (A5).

### References

Allen, C.R., Amand, P.S., Richter, C. and Nordquist, J., 1965. Relationship between seismicity and geologic structure in Southern California. *Bull. Seismol. Soc. Am.*, 55: 753–797.

Bak, P. and Tang, C., 1989. Earthquakes as a self-organized critical phenomenon. *J. Geophys. Res.*, 94: 15 635–15 637.

Carlson, J.M. and Langer, J.S., 1989. Properties of earthquakes generated by fault dynamics. *Phys. Rev. Lett.*, 62: 2632–2635.

Cochard, A. and Madariaga, R., 1994. Dynamic faulting under rate-dependent friction. *Pure Appl. Geophys.*, 142: 419–445.

Ellsworth, W.L. and Beroza, G.C., 1995. Seismic evidence for an earthquake nucleation phase. *Science*, 268: 851–855.

Fedotov, S.A., 1965. Regularities in the distribution of strong earthquakes in Kamchatka, the Kurile Islands, and northeastern Japan. *Tr. Inst. Fiz. Zemli, Akad. Nauk.*, 36: 66–93 (in Russian).

Kame, N., 1995. Initial process of dynamic earthquake faulting – How do crack interactions affect it? Masters Thesis, University of Tokyo (in Japanese).

Kame, N. and Yamashita, T., 1996. Dynamic nucleation process of shallow earthquake faulting in a fault zone. Submitted to *Int. J. Geophys.*

Kostrov, B.V., 1966. Unsteady propagation of longitudinal shear cracks. *J. Appl. Math. Mech.*, 30: 1241–1248.

Leary, P.C., Li, Y.-G. and Aki, K., 1987. Observation and modelling of fault-zone fracture seismic anisotropy, I. P, SV and SH travel times. *Geophys. J. R. Astron. Soc.*, 91: 461–484.

Madariaga, R., 1977. High-frequency radiation from crack (stress drop) models of earthquake faulting. *Geophys. J. R. Astron. Soc.*, 51: 625–651.

Madariaga, R., 1983. High-frequency radiation from dynamic earthquake models. *Ann. Geophys.*, 1: 17–23.

Mogi, K., 1963. Some discussions of aftershocks, foreshocks and earthquake swarms. *Bull. Earthquake Res. Inst.*, 41: 615–658.

Mogi, K., 1969. Some features of recent seismic activity in and near Japan (2): Activity before and after great earthquakes. *Bull. Earthquake Res. Inst.*, 47: 395–417.

Ohtake, M., 1976. Search for precursors of the 1974 Izu-Hanto-Oki earthquake, Japan. *Pure Appl. Geophys.*, 114: 1083–1093.

Ohtake, M., Matsumoto, T. and Latham, G.V., 1977. Seismic gap near Oaxaca, Southern Mexico, as a possible precursor to a large earthquake. *Pure Appl. Geophys.*, 115: 375–385.

- Rice, J.R., 1992. Fault stress state, pore pressure distributions, and the weakness of the San Andreas Fault, In: E.B. Evans and T.F. Wong (Editors), *Fracture Mechanics and Transport Properties of Rocks*. Academic Press, London, pp. 475–503.
- Rice, J.R., 1993. Spatio-temporal complexity of slip on a fault. *J. Geophys. Res.*, 98: 9885–9907.
- Segall, P. and Pollard, D.D., 1980. Mechanics of discontinuous faults. *J. Geophys. Res.*, 85: 4337–4350.
- Sih, G.C., 1965. Stress distribution near internal crack tips for longitudinal shear problems. *J. Appl. Mech.*, 32: 51–58.
- Umeda, Y., 1981. An earthquake source model with a ripple generating core. *J. Phys. Earth*, 29: 341–370.
- Umeda, Y., 1990. High-amplitude seismic waves radiated from the bright spot of an earthquake. *Tectonophysics*, 175: 81–92.
- Umeda, Y., 1992. The bright spot of an earthquake. *Tectonophysics*, 211: 13–22.
- Umeda, Y., Kuroiso, A., Ito, K. and Muramatsu, I., 1987. High accelerations produced by the western Nagano prefecture, Japan, earthquake of 1984. *Tectonophysics*, 141: 335–343.
- Umeda, Y., Ito, K., Kato, M. and Arboleda, R.A., 1991. Thrown-out stones by the 1990 Philippine earthquake. *Annals Disas. Prev. Res. Inst.*, 34: 1–9 (in Japanese).
- Yamashita, T., 1983. High-frequency acceleration radiated by unsteadily propagating cracks and its near-source geometrical attenuation. *J. Phys. Earth*, 31: 1–32.
- Yamashita, T., 1993. Application of fracture mechanics to the simulation of seismicity and recurrence of characteristic earthquakes on a fault. *J. Geophys. Res.*, 98: 12,019–12,032.
- Yamashita, T., 1995. Simulation of seismicity due to ruptures on non-coplanar interactive faults. *J. Geophys. Res.*, 100: 8339–8350.
- Yamashita, T. and Fukuyama, E., 1996. Apparent critical slip displacement caused by the existence of a fault zone. *Geophys. J. Int.*, 125: 459–472.
- Yamashita, T. and Knopoff, L., 1989. A model of foreshock occurrence. *Geophys. J. Int.*, 96: 389–399.
- Yamashita, T. and Knopoff, L., 1992. Model for intermediate-term precursory clustering of earthquakes. *J. Geophys. Res.*, 97: 19,873–19,879.
- Yamashita, T. and Umeda, Y., 1994. Earthquake rupture complexity due to dynamic nucleation and interaction of subsidiary faults. *Pure Appl. Geophys.*, 143: 89–116.
- Zeng, Y., Aki, K. and Teng, T., 1993. Mapping of the high-frequency source radiation for the Loma Prieta earthquake, California. *J. Geophys. Res.*, 98: 11 981–11 993.